*Article*

JOURNAL OF ELASTOMERS & PLASTICS

Journal of Elastomers & Plastics
1–15

DOI: 10.1177/0095244312469965
jep.sagepub.com
SAGE

# Compatibility of hydrazine and EPDM rubber containing polybutadiene coagent

**Ping Li[1], Fernando Aguirre[2], Michael O Killpack[1], Stephen L Rodgers[3] and Ian A Ballinger[4]**

## Abstract

Histogram analyses of atomic force microscopy (AFM) phase images demonstrated changes in the surface composition of ethylene propylene diene–modified (EPDM) elastomeric formulations containing polybutadiene after exposure to hydrazine. It was determined by Fourier-transform infrared (FT-IR) spectroscopic analysis that the change in the surface composition is caused by hydrogenation of the vinylic double bonds of the polybutadiene coagent, stemming from diimide generation from hydrazine. The diffusion and subsequent reaction of hydrazine with two cured EPDM elastomeric formulations were investigated by mapping FT-IR spectroscopy. The depth of diffusion and reaction was determined by monitoring changes in the intensity of the vinyl group signal from the polybutadiene in the FT-IR spectra. The FT-IR analysis of horizontal microtome specimens and vertical 'cross section' of the EPDM samples showed that hydrazine diffused less than 200 μm into the elastomeric materials over a period of 40 weeks. Sequential proton nuclear magnetic resonance spectroscopy of the polybutadiene coagent showed that the vinyl groups in polybutadiene were hydrogenated when mixed with hydrazine at room temperature. The reaction of hydrazine with the polybutadiene coagent of the EPDM elastomeric material was corroborated by matrix-assisted laser desorption/ionization time of flight mass spectrometry as well. A model compound, 4-vinyl cyclohexene, was used to assess the relative hydrogenation rate of primary and secondary double bonds using gas chromatography/mass spectrometry.

[1] Research and Development, ATK Aerospace Systems, Brigham City, UT, USA
[2] Fresenius Medical Care, Ogden, UT, USA
[3] AFRL/RQR, Rocket Propulsion Division, Edwards AFB, CA, USA
[4] Space Structures and Components, ATK Aerospace Systems, Commerce, CA, USA

**Corresponding author:**
Ping Li, Research and Development, ATK Aerospace Systems, Brigham City, UT 84302, USA
Email: Ping.Li@ATK.com

**Keywords**
EPDM, AFM, FT-IR, MALDI-TOF, GC/MS, NMR

## Introduction

Ethylene propylene diene–modified (EPDM) rubber is a thermoplastic elastomer widely used in the automotive industry because of its low cost, low specific gravity and ease of processability.[1,2] In the aerospace industry, EPDM elastomeric materials have been used in low-cost, light weight diaphragms and bladders in hydrazine propellant tanks.[3] The EPDM rubber's physical and chemical stability are typically enhanced using liquid polyfunctional polymers as coagents to increase cross-linking in the systems.[4,5] When EPDM elastomer containing 1,2-polybutadiene coagents is cured with peroxide catalysts, the resulting product is heat, corrosion and hydrocarbon resistant. Cray Valley reported that small amounts of 1,2-polybutadiene, as low as 2.5 phr, have significant effects on compression and hardness in peroxide-cured EPDM elastomers.[1] Higher concentrations of 1,2-polybutadiene resins can result in improved heat, chemical and oil resistance.

Over the years, an EPDM elastomeric material identified as AF-E-332 has shown a successful flight heritage in diaphragms and bladders in hydrazine propellant tanks.[3] However, due to obsolescence issues with the EPDM rubbers used in the AF-E-332, a new formulation named SIFA has recently been developed using alternative EPDM rubbers.[4] The new SIFA material contains 1,2-polybutadiene coagent, a fluoropolymer and inorganic fillers. Mechanical testing and diaphragm processing of the new SIFA showed that this material retained the manufacturability and performance of AF-E-332 diaphragms.[5]

The purpose of this study was to develop an improved methodology to monitor surface property change and diffusion of hydrazine into AF-E-332 and SIFA. Changes in the surface property were monitored by atomic force microscopy (AFM), while diffusion of hydrazine was monitored by Fourier-transform infrared (FT-IR) analysis of horizontally microtomed specimens and vertical 'cross-sectional' specimens of EPDM. The long-term stability and hydrazine compatibility of the EPDM rubber was studied by immersing samples in hydrazine at 70°C for a period of time using several analytical techniques. The results provide a better understanding of the EPDM rubber–hydrazine interaction which is essential to avoid performance degradation of hydrazine propellant tanks.

## Experimental section

### Materials

Samples of cured AF-E-332 and SIFA as well as their individual components including 1,2-polybutadiene, EPDM elastomer, fluoropolymer and inorganic filler were supplied by ATK Space Structures and Components (Commerce, California, USA). Hydrazine was supplied from United Space Alliance (Cape Canaveral, Florida, USA). Tetrahydrofuran (THF) was obtained from Aldrich (Milwaukee, Wisconsin, USA). All *trans*-retinoic acid and copper (I) iodide (CuI) salt were acquired from Alfa Aesar (Ward Hill,

Massachusetts, USA). Deuterated THF ($d_8$-THF) and 4-vinyl cyclohexene (VCH) were obtained from Aldrich (St. Louis, MO, USA). All materials were used as received.

## Elastomer aging

Small samples (approximately 50 mm in diameter and 3 mm in thickness) of AF-E-332 and SIFA were cut and placed in 250 mL glass flasks. Hydrazine (approximately 50 mL) was added to each flask, sealed and then heated in an oven at 70°C. These EPDM samples were analyzed every 6 weeks up to 40 weeks. The solid AF-E-332 and SIFA samples were removed from the hydrazine and washed with deionized water and air dried at 25°C.

## Sample preparation for MALDI-TOF analysis

Samples of uncured EPDM and 1,2-polybutadiene were solvated in THF at 5 mg/mL and combined with CuI (10 mg/mL in $H_2O$) and retinoic acid matrix (25 mg/mL in THF) in a 1:1:2 ratio. All the chemicals were used without further purification.

## Sample preparation for NMR spectroscopy and GC/MS

Two solutions of 1,2-polybutadiene/hydrazine were prepared by mixing an aliquot of a 2 wt% 1,2-polybutadiene in $d_8$-THF with hydrazine (10 wt% and 50 wt% solutions of $d_8$-THF). The samples were kept at ambient temperature (20–27°C) and tested fresh (zero time), 2, 5 and 7 days, respectively. Three additional solutions were prepared consisting of a 2 wt% VCH in $d_8$-THF containing 0, 10, 20 and 50 wt% hydrazine.

## AFM analysis

A piece of EPDM rubber (approximately 5 × 3 × 2 mm) was placed onto a standard glass microscope slide. The sample was bonded to the glass slide using Hardman® Double Bubble® Urethane D-50 adhesive (Belleville, NJ, USA). The AFM images of the EPDM rubber's surface were obtained with an Asylum Research MFP-3D™ stand-alone microscope under ambient conditions. The microscope was equipped with a Table Stable TS-150 vibration isolation table and a Herzan AEK 2002 vibration isolation hood. The images were obtained using the MFP-3D controller and Igor Pro MFP3D software. The AFM images were collected in intermittent contact (tapping) mode using a standard silicon cantilever having a spring constant of approximately 1.3 N/m and a drive frequency of approximately 60 kHz. The set point amplitudes were between 20% and 50% of the cantilever's free amplitude. The AFM images were collected with a scan rate of 0.5 Hz and a resolution of 512 × 512 pixels. High-resolution images were collected at the same scan rate but with 1,024 × 1,024 pixel resolution.

## Microtome and cross-section sampling

Cured EPDM materials were bonded on wooden blocks using Hardman Double Bubble Urethane D-50 adhesive. The samples were cooled in a freezer at −10°C for 2 h and then

fitted in an AO-860 microtome clamp. Several specimens approximately 200 μm thick were obtained by horizontally microtoming the EPDM samples for FT-IR spectroscopic studies. A cross section of the each EPDM sample, approximately 3 mm thick, was microtomed at 90° for FT-IR microscopic studies.

## FT-IR analysis

FT-IR spectra of microtomed samples were collected in a Nicolet 6700 spectrometer. The samples were clamped on a single-bounce attenuated total reflection (ATR) Ge crystal. The FT-IR spectra contain 128 scans collected between 4,000 $cm^{-1}$ and 650 $cm^{-1}$, with 8 $cm^{-1}$ resolution. FT-IR spectra were collected on the AF-E-332 and SIFA samples prior to and after exposure to hydrazine. The FT-IR mapping of the cross-sectional samples was performed in a Nicolet Magna 670 FT-IR spectrophotometer using an infinity series diamond ATR objective. The microscope was equipped with a video camera and a liquid nitrogen-cooled mercury cadmium telluride detector. FT-IR mapping of the EPDM samples was done in a grid pattern with the computer-controlled microscope stage and the Atlas software package. An approximately 3,000 × 500 $\mu m^2$ area of the cross section was mapped using a beam spot size of 150 × 150 μm and a step size of 50 μm. At each point, an FT-IR spectrum was collected between 4,000 $cm^{-1}$ and 650 $cm^{-1}$, with a spectrum resolution of 8 $cm^{-1}$ and 64 scans. The absorbance maps were processed using the heights of the vinyl peak at 910 $cm^{-1}$ of 1,2-polybutidene and normalized to the unchanged C–F stretching signal at 1,230 $cm^{-1}$ of the fluoropolymer in the AF-E-332 and SIFA.

## MALDI-TOF MS analysis

A Waters® Synapt™ matrix-assisted laser desorption/ionization time of flight (MALDI-TOF) mass spectrometer with a 9 kV reflectron flight tube was used for the analysis. The MALDI source employed a Lumanova® 355 nm nitrogen laser, with 3 ns pulse widths, fired at 200 Hz. The laser energy was held constant slightly above the ion detection threshold at ≤100 μJ/pulse. Ions were detected with a microchannel plate detector held at −1700 V. All the polymer signals were detected in the positive mode as copper-ion adducts in the form $(M + Cu)^+$ from the addition of CuI to the sample matrix. The collisional cooling gas flow at the source was maintained at 2.5 mL/h. The quadrupole trap gas was adjusted to maintain the trap pressure between 5.3 and 5.8 × $10^{-3}$ mbar. Summed spectra from 3 min of manual scan at *m/z* 400–8,000 were processed for each sample using MassLynx™ v4.1 software.

## NMR spectroscopic analysis

Nuclear magnetic resonance (NMR) spectra were collected with a JEOL Eclipse 400 MHz spectrometer. The spectra are reported in parts per million relative to the proton signal from tetramethylsilane ($(CH_3)_4Si$).

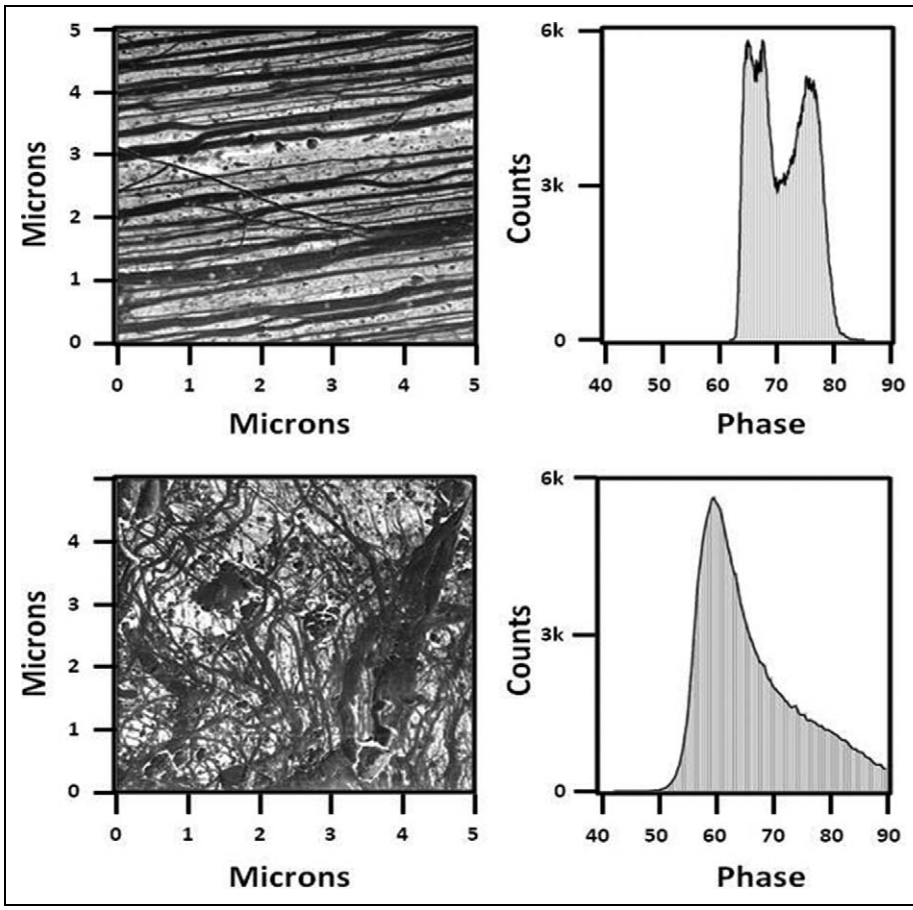


**Figure 1.** AFM phase images (left) and histogram (right) of AF-E-332 elastomeric material prior to (top) and after exposure (bottom) to hydrazine. AFM: atomic force microscopy.

### *GC/MS analysis*

An Agilent gas chromatography/mass spectrometry (GC/MS) system with a DB-5 column was used for the analysis. Helium was used as the carrier gas with a flow rate of 1.0 mL/min with a 50 split ratio.

## Results and discussion

### *AFM analysis*

AFM has been effectively used to map heterogeneous regions in several multicomponent polymer blends.[6] In particular, polymer domains have been studied using the color

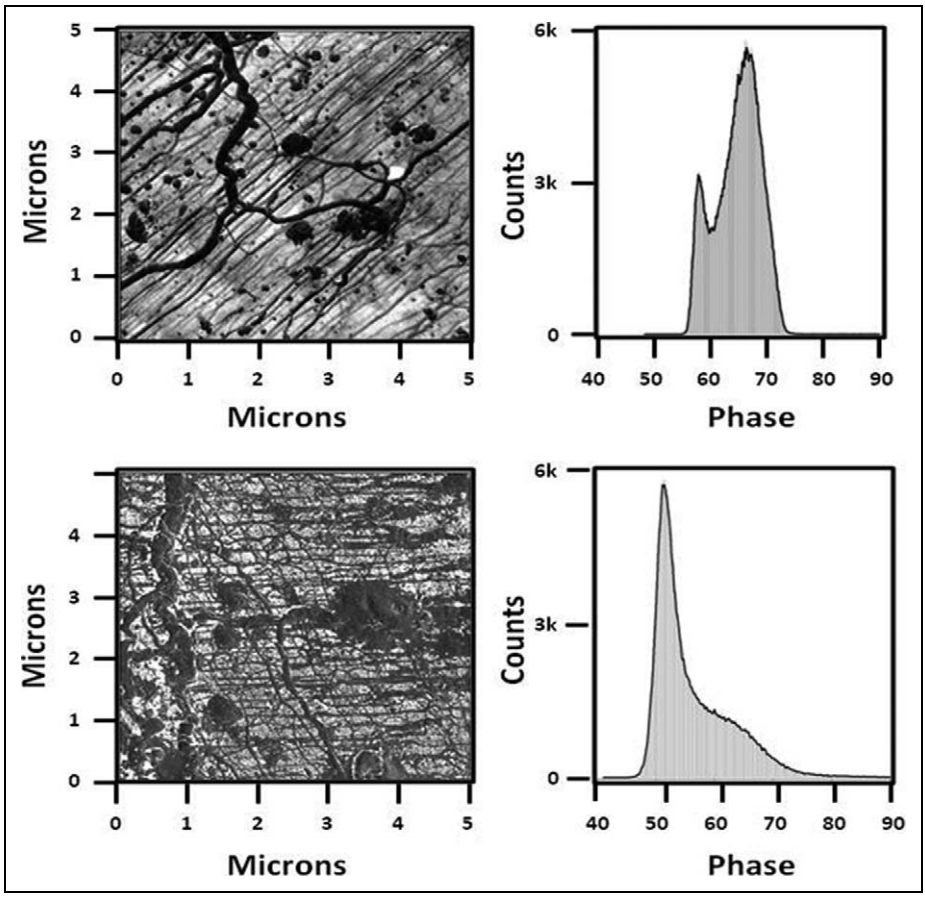


**Figure 2.** AFM phase images (left) and histogram (right) of SIFA elastomeric material prior to (top) and after (bottom) exposure to hydrazine. AFM: atomic force microscopy.

contrast in phase images that is produced by the interactions between the AFM tip and different regions of the sample surface having different chemical and mechanical properties. Cleveland et al.[7] have shown that color contrast in a phase image is related to energy dissipation at the tip–sample junction. However, this method is not satisfactory for assigning chemical composition and so complementary chemical analysis is necessary for this purpose.[6,8] Figures 1 and 2 show the phase images recorded for the surface of AF-E-332 and SIFA prior to (top) and after (bottom) exposure to hydrazine. The images of the material prior to exposure to hydrazine show dark striations in a bright surrounding matrix. Previous studies have assigned the dark regions to harder material and the lighter region to softer material.[8] Therefore, the dark color striations indicate that less energy was dissipated in these domains than in the bright matrix. Force–distance curves measured on the moieties in Figure 1 confirmed that the dark striations are stiffer

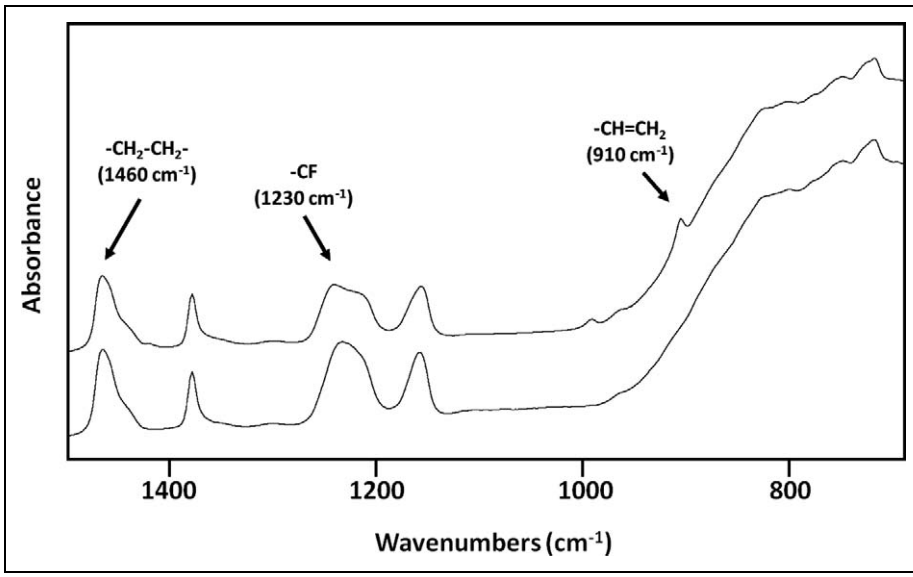


**Figure 3.** FT-IR spectrum of cured SIFA prior to (top) and after (bottom) exposure to hydrazine for 6 weeks. FT-IR: Fourier-transform infrared.

than the domains in the bright matrix. The parallel arrangement of the dark domains before hydrazine exposure was significantly distorted after the samples were introduced to hydrazine. This implies that the random pattern must be a consequence of the diffusion of hydrazine into the elastomer. The histograms on the right of Figures 1 and 2 show the distribution of dark and bright domains in the phase images of AF-E-332 and SIFA prior to (top) and after (bottom) exposure to hydrazine. The histograms from the images recorded prior to exposure to hydrazine show multiple distinct peaks at different phase values. This change in the shape of the histograms suggests that the surface composition of both the AF-E-332 and SIFA was significantly changed after they were exposed to hydrazine. The shifting of the histogram distributions to lower phase values suggests that the surfaces of the elastomeric material became stiffer after they were exposed to hydrazine. However, the surface property change did not result in the observation of any surface cracks or blister formation on these EPDM samples.

## *FT-IR spectroscopic analysis*

Figure 3 shows the FT-IR spectra (absorbance mode) of SIFA—prior to (top) and after (bottom) exposure to hydrazine. The spectrum of neat material shows characteristic signal of the C–C stretching bands of EPDM at 1,460 $cm^{-1}$ as well as the vinyl group ($–CH=CH_2$) stretch from 1,2-polybutadiene at 910 $cm^{-1}$. The 1,2-polybutadiene peaks of the SIFA are overlapped with the signal from inorganic fillers that produces the increase in the baseline signal at lower wave numbers. The spectra also show the

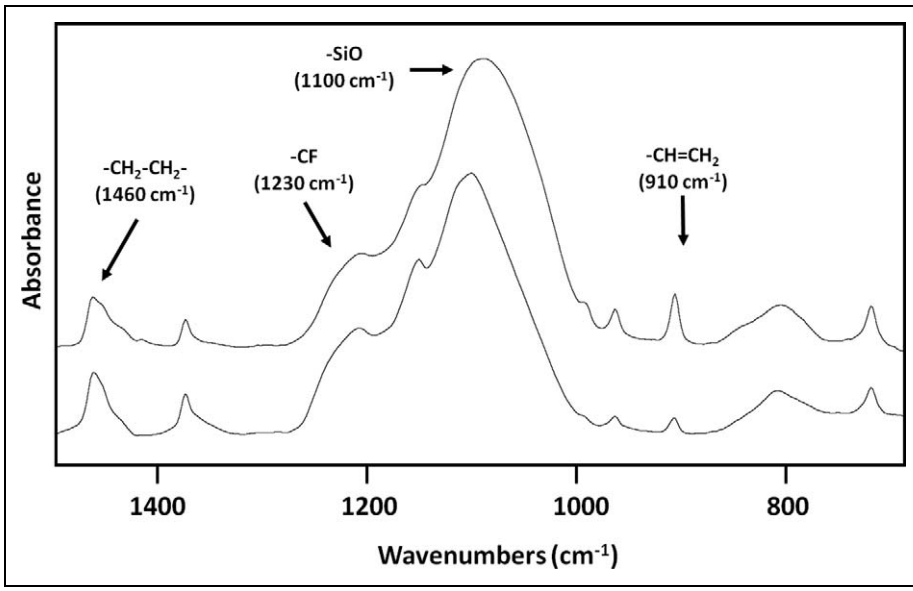


**Figure 4.** FT-IR spectrum of cured AF-E-332 prior to (top) and after (bottom) exposure to hydrazine for 6 weeks. FT-IR: Fourier-transform infrared.

characteristic fluoropolymer signal (–CF) at 1,230 $cm^{-1}$. In contrast, the vinyl group signal is not observed in the spectrum of SIFA after exposure to hydrazine. This suggests that the 1,2-polybutadiene in the SIFA either reacted with hydrazine or leached out from the surface. The possibility of the polybutadiene leaching is unlikely because it is expected that some of the vinyl groups in polybutadiene have chemically anchored the polymer chains to the EPDM rubber. Figure 4 shows the FT-IR spectra of AF-E-332 prior to (top) and after (bottom) exposure to hydrazine. The spectra show the same characteristic signals of 1,2-polybutadiene, EPDM rubber and fluoropolymer as previously described for SIFA. The dominant peak at 1,100 $cm^{-1}$ arises from silicon-based filler. Similar to the SIFA, the intensity of the signal at 910 $cm^{-1}$ corresponding to the vinyl group of 1,2-polybutadiene was significantly reduced after the material was exposed to hydrazine.

In order to investigate the diffusion of hydrazine into the AF-E-332 and SIFA, several microtome samples, approximately 200 μm thick, were cut from samples exposed to hydrazine at 70°C. The FT-IR analysis of these samples was performed every 6 weeks up to 40 weeks. Figure 5 shows the variation in intensity of the vinyl group signal in the FT-IR spectra from the microtomed specimens exposure to hydrazine for 6 weeks. The vinyl signal was normalized to the C–F signal from the fluoropolymer in the samples at 1,230 $cm^{-1}$ which remains constant. It is evident that the vinyl signal is significantly reduced in the first slice corresponding to the surface of the SIFA and AF-E-332 exposed to hydrazine. Based on the FT-IR response at 910 $cm^{-1}$, 95% vinyl group of

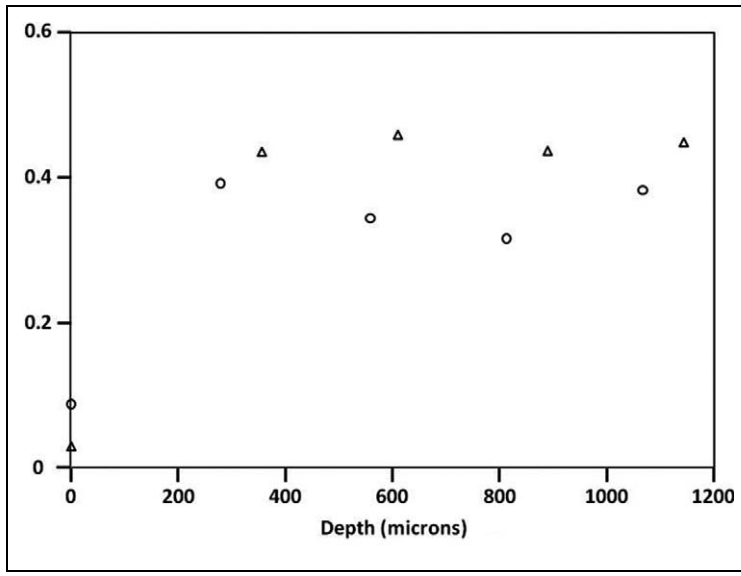


**Figure 5.** Variation in intensity of the vinyl group signal (910 $cm^{-1}$) in microtome slices from SIFA (O) and AF-E-332 (Δ) materials after exposure to hydrazine.

1,2-polybutadiene on the surface of SIFA and 80% on the surface of AF-E-332 were hydrogenated from hydrazine during the first 6 weeks at 70°C. The signal remains relatively unchanged from microtome slices taken from the bulk of the materials. The variation in the vinyl signal suggests that hydrazine penetrates less than 200 μm into the elastomer.

Imada et al. reported that olefins can be hydrogenated with hydrazine in the presence of a perchlorate catalyst under an oxygen atmosphere.[9] To determine the dependence of the reduction in the presence of oxygen, hydrogenation of the EPDM formulations in the absence of oxygen was evaluated. Both the SIFA and AF-E-332 samples were immersed in hydrazine and purged with argon to eliminate oxygen. It was determined by FT-IR spectroscopy that the vinyl groups in both formulations were chemically reduced after 4 weeks at 70°C as evidenced by the disappearance of the vinyl peak at 910 $cm^{-1}$. These results clearly indicated that hydrazine hydrogenation in the studied EPDM formulations is selfcatalyzed. Therefore, FT-IR spectroscopy is an effective tool to detect hydrazine penetration in the EPDM to monitor the change in the vinyl signal at 910 $cm^{-1}$.

## *FT-IR microscopic analysis*

FT-IR microscopy is an important technique in the analysis of industrial materials, because it combines the spatial specificity of microscopy with the powerful chemical specificity of spectroscopy.[10,11] The technique has been widely used to determine the additives, contaminants, curing processes and degradation of multiple polymer systems.[12,13] Figure 6 shows the FT-IR color contour maps of vertical cross-section samples

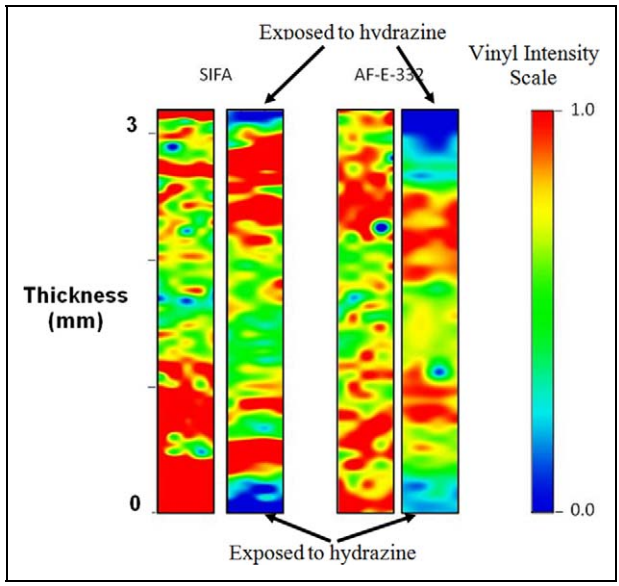


**Figure 6.** FT-IR microscopy color contour maps obtained by measuring the intensity of the vinyl group signal (910 $cm^{-1}$) from AF-E-332 and SIFA prior to (left) and after (right) exposure to hydrazine. On the intensity scale, red equals maximum vinyl signal intensity and blue equals no vinyl signal detected. FT-IR: Fourier-transform infrared.

of AF-E-332 and SIFA prior to (left) and after (right) immersion in hydrazine. The sample with 3 mm thickness was exposed to hydrazine from both sides. The maps show the variation in the intensity of the vinyl group signal at 910 $cm^{-1}$ from the 1,2-polybutadiene in the EPDM formulations. Similar to the analysis of the microtome slices, the 1,2-polybutadiene signal was normalized to the constant C–F signal at 1,230 $cm^{-1}$ from the fluoropolymer in the samples. The color contour map of the cross section of the SIFA and AF-E-332 samples shows a significant reduction in the intensity of the vinyl group within approximately 200 μm from both surfaces (top and bottom) exposed to hydrazine. The FT-IR signal of the vinyl group remains strong when moving away from the surfaces into the bulk material. The results from the color contour maps are consistent with the penetration of hydrazine observed from the analysis of microtome slices from SIFA and AF-E-332 samples previously discussed.

## *MALDI-TOF mass spectroscopic analysis*

FT-IR analysis of cured EPDM material showed that the 1,2-polybutadiene vinyl group signal decreased after the sample was immersed in hydrazine at 70 C. To further characterize this interaction, MALDI-TOF was used to characterize the mechanism and products formed from the reaction of 1,2-polybutadiene with hydrazine. Table 1 lists the

**Table 1.** 1,2-polybutadiene/hydrazine samples analyzed by MALDI-TOF MS

| Sample ID | 1 | 2 | 3 | 4 | 5 | 6 |
|---|---|---|---|---|---|---|
| | 1,2-polybutadiene/hydrazine ratio in THF solutions | | | | | |
| % 1,2-polybutadiene | 100 | 0 | 99 | 90 | 80 | 50 |
| % hydrazine | 0 | 100 | 1 | 10 | 20 | 50 |

MALDI-TOF: matrix-assisted laser desorption/ionization time of flight; THF: tetrahydrofuran.

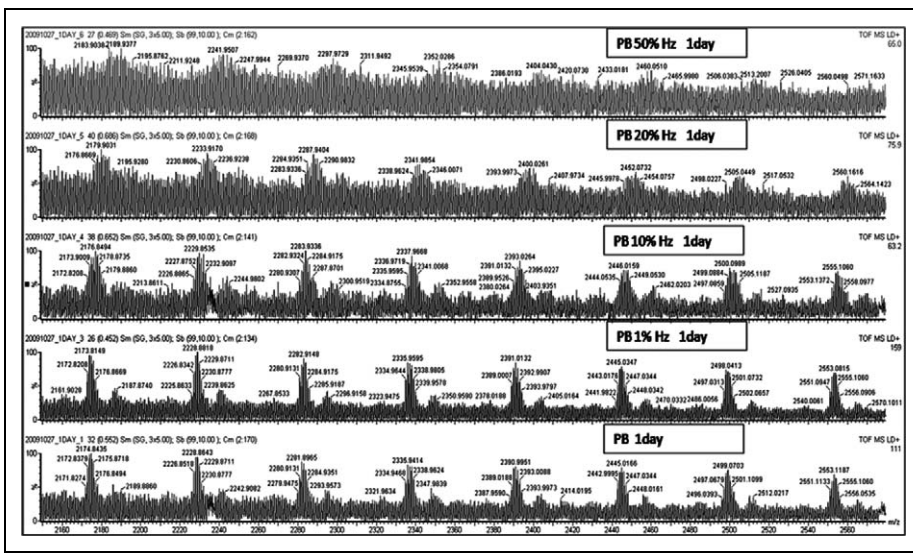


**Figure 7.** Positive MALDI-TOF MS spectra of 1,2-polybutadiene/hydrazine samples after 1 day at ambient conditions. MALDI-TOF MS: matrix-assisted laser desorption/ionization time of flight mass spectrometry.

composition of the 1,2-polybutadiene/hydrazine samples. All the samples were kept at ambient conditions and analyzed at zero time and after 1 and 4 days.

Figure 7 shows a characteristic MALDI-TOF mass spectrum of 1,2-polybutadiene. The spectrum shows a series of peaks separated by a $\Delta m/z = 54$ characteristic of the butadiene-repeating units. The mass spectra of the 1,2-polybutadiene/hydrazine samples conditioned after 1 and 4 days also show a $\Delta m/z = 54$ at time zero. However, after 1 day at ambient conditions, the sample containing 50% hydrazine shows a broader molecular weight distribution of the polymer peak and a $m/z = 14$–$16$ shift to the higher molecular weight. However, the sample containing 10% hydrazine shows a $m/z = 2$ shift after 1 day at ambient conditions. After 4 days at ambient conditions, the signal from the sample containing 10% hydrazine shows a $m/z = 12$ shift while the $\Delta m/z = 54$ characteristic of the butadiene-repeating units disappeared for the sample containing 50% hydrazine. The shift in molecular weight $\Delta m/z = 14$ and 16 as well as the disappearance of the

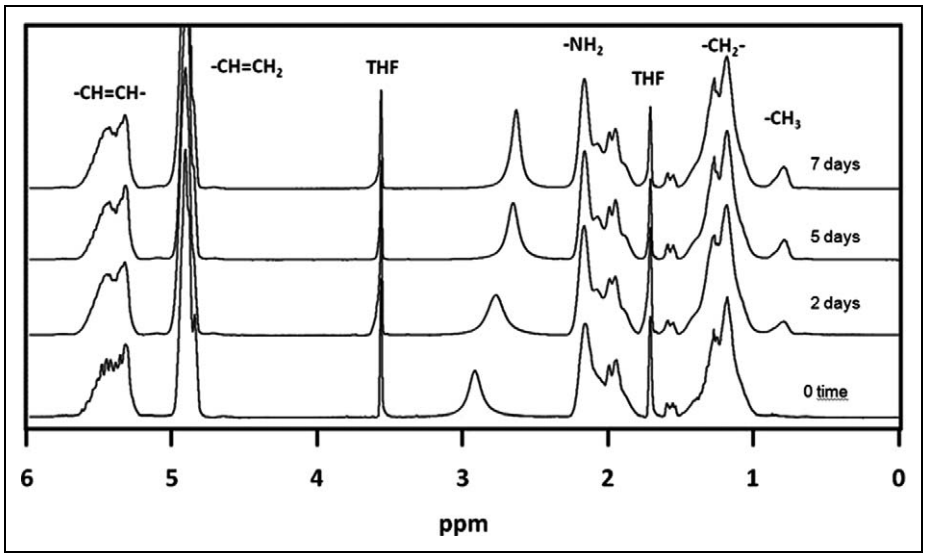


**Figure 8.** $^1$H-NMR spectra of a 1,2-polybutadine/hydrazine solution in $d_8$-THF maintained at ambient condition for 0, 2, 5 and 7 days. $^1$H-NMR: proton nuclear magnetic resonance; $d_8$-THF: deuterated tetrahydrofuran.

polybutadiene signal in the MALDI-TOF spectra is an indication of the reaction of hydrazine with polybutadiene as previously suggested in the FT-IR section. The MALDI-TOF spectra of samples containing high levels of hydrazine showed a lower signal-to-noise (S/N) ratio than the spectrum of polybutadiene without hydrazine. This S/N reduction is most likely due to the lower MALDI-TOF efficiency to ionize polymers with a reduced number of unsaturated chains. Figure 7 shows the MALDI-TOF signal of the 1,2-polybutadiene after 1 day with hydrozine in THF.

## *$^1$H-NMR spectroscopic analysis*

Transfer hydrogenation of alkenes and unsaturated polymers by treatment with hydrazine and its derivates has been previously studied. The reaction proceeds via a diimide (HN=NH) hydrogen transfer agent derived from hydrazine.[14–16] The diimide is an active intermediate that coordinates with the unsaturated group prior to adding two hydrogen across the C=C bond. Figure 8 shows a time elapsed series of proton NMR ($^1$H-NMR) spectra collected on a sample of 1,2-polybutadiene containing 10% hydrazine that was maintained at ambient conditions for 7 days. The NMR spectra show characteristic proton peaks of methylene groups (–$CH_2$–; 1.2 and 1.9 ppm), 1-ethylene groups from the backbone (–CH=CH–; 5.5 ppm), and vinyl groups (–CH=$CH_2$; 4.9 ppm) of polybutadiene. Other peaks include the amine group (–$NH_2$; 2.2 ppm) of hydrazine and the methylene groups (–$CH_2$–; 1.7 and 3.6 ppm) of

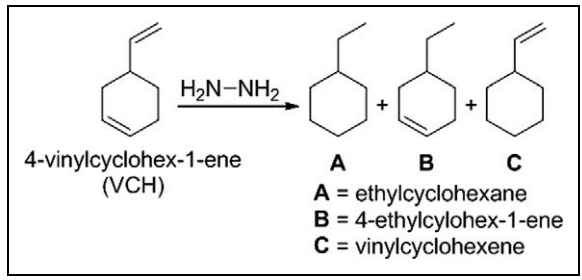


**Figure 9.** Reaction of VCH with hydrazine showing the three possible reaction products. Compounds A and B were experimentally observed. VCH: 4-vinyl cyclohexene.

**Table 2.** Relative concentration of VCH and hydrogenation reaction products after 3 days' exposure to hydrazine at ambient conditions

| | Relative concentration (%) using peaks areas | | | |
|---|---|---|---|---|
| Sample description | VCH | 4-ethylcyclohex-1-ene | Vinylcyclohexane | Ethylcyclohexane |
| VCH + 0% hydrazine | >98 | 0.4 | ND | ND |
| VCH + 10% hydrazine | 74.6 | 25.1 | 0.2 | ND |
| VCH + 50% hydrazine | 80.1 | 19.7 | 0.2 | ND |

VCH: 4-vinyl cyclohexene; ND: none detectable.

THF. The $^{1}$H-NMR spectra show that the intensity of a methyl group ($-CH_3$) at $\delta$ 0.90 ppm increased while that for the vinyl group at $\delta$ 4.9 ppm decreased over time. In addition, the $^{1}$H-NMR spectra show a progressive upfield shift in the peak at 2.9 ppm. Overtime, the intensity of the peak increases, while the full-width half-maximum narrows.[17] These changes in the NMR spectra indicate that the vinyl groups of polybutadiene undergo reduction when exposed to hydrazine. These results are in agreement with the previously discussed diffusion of hydrazine into AF-E-332 and SIFA monitored by FT-IR spectroscopy.

## *GC/MS analysis*

Mango and Lenz determined that the diimide hydrogenation rates of vinyl groups are faster than the rates for *cis*- and *trans*-units.[18–20] In this study, the hydrogenation rate for primary and secondary C=C double bonds was investigated using a model compound VCH. Samples of VCH, containing 0%, 10% and 50% hydrazine by volume, were analyzed by GC/MS. Figure 9 shows three potential reaction products (vinylcyclohexane, 4-ethylcyclohex-1-ene and ethylcyclohexane) from the hydrogenation of VCH with hydrazine. Two of the predicted reaction products, 4-ethylcyclohex-1-ene and vinylcyclohexane, were observed as identified by GC/MS. The GC/MS results corroborate that

the vinyl group in VCH is hydrogenated when exposed to hydrazine. In addition, hydrogenation of the double bond in the cyclohexene ring occurred at a significantly lower relative rate compared to the vinyl group. The relative amounts of the observed reaction products are listed in Table 2.

The reaction of hydrazine with the model compound (VCH) indicates that the hydrogenation rate for secondary C=C double bonds is about 100 times less than that for primary C=C double bonds. These results also show that the secondary C=C double bonds along the polybutadiene backbone in EPDM can be completely hydrogenated by hydrazine leading to improved resistance of EPDM to heat and oxidation.

## Conclusions

Histogram analyses of phase AFM images of AF-E-332 and SIFA determined changes in their surface compositions after exposure to hydrazine. However, these changes did not cause any surface cracks and blisters of the EPDM formulations which are the common compatibility concerns of the EPDM/hydrazine applications. It was also determined by FT-IR spectroscopy that the polybutadiene coagent in AF-E-332 and SIFA, used in the diaphragms and bladders of monopropellant tanks, is hydrogenated by exposure to hydrazine. FT-IR spectroscopy analysis of horizontal microtomed EPDM samples from the hydrazine exposed surface and FT-IR microscopic mapping of cross-sectional samples showed hydrogenation of polybutadiene within 200 μm from the surface of AF-E-332 and SIFA exposed to hydrazine. The FT-IR analyses proved to be an effective methodology to monitor the diffusion of hydrazine into the elastomeric materials. The results were supported by $^{1}$H NMR spectroscopy, MALDI-TOF MS and GC/MS. In addition, this study showed that the exposure of EPDM elastomer to hydrazine does not detrimentally affect the properties of the elastomer and in fact reduces the reactive C=C double bonds in the surface which could lead to improved thermal and oxidative stability of the elastomeric material.

### Acknowledgement

Shawn Parry, Max Patterson, Bart Webber and Joanne Bingham of ATK Aerospace Systems, are gratefully acknowledged for collecting the MALDI-TOF MS, NMR, GC/MS and FT-IR data respectively.

### References

1. Cray Valley. *Liquid 1,2 polybutadiene resins as co-agents for EPDM*. Application Note 5710. Exton, PA: Cray Valley USA.
2. Cray Valley. *Selecting co-agents for use in peroxide-cured elastomers*. Application Note 5719. Exton, PA: Cray Valley USA.
3. Ballinger IA, Lay WD and Tam WH. Review and history of PSI elastomeric diaphragm tanks. In: *31st AIAA/ASME/SAE/ASEE joint propulsion conference and exhibit*, San Diego, CA, USA, 10-12 July 1995, paper no. AIAA 95-2534. Reston, VA: American Institute of Aeronautics and Astronautics.

4. Ballinger IA and Sims D. Development of an EPDM elastomeric material for use in hydrazine propulsion systems. In: *39th AIAA propulsion conference*, Huntsville, AL, USA, 21 July 2003, paper no. AIAA 2003-4611. Reston, VA: American Institute of Aeronautics and Astronautics.
5. Tam WH, Ballinger IA and Kohorst P. Design and manufacture of a composite overwrapped elastomeric diaphragm tank. In: *40th AIAA/ASME/SAE/ASEE joint propulsion conference and exhibit*, Fort Lauderdale, FL, USA, 11–14 July 2004, paper no. AIAA 2004-3507. Reston, VA: American Institute of Aeronautics and Astronautics.
6. Pfau A, Janke A and Heckmann W. Determination of the bulk structure of technical multi-phase polymer systems with AFM: comparative AFM and TEM investigation. *Surf Interface Anal* 1999; 27: 410–417.
7. Cleveland JP, Anczykowski B, Schmid AE and Elings VB. Energy dissipation in tapping-mode atomic force microscopy. *Appl Phys Lett* 1998; 72: 2613–2615.
8. Bar G, Thomann Y, Brandsch R, Cantow HJ and Whangho MH. Tapping mode atomic force microscopy. *Langmuir* 1997; 13: 3807–3812.
9. Imada Y, Iida H and Naota T. Flavin-catalyzed generation of diimide: an environmentally friendly method for the aerobic hydrogenation of olefins. *J Am Chem Soc* 2005; 127: 14544–14545.
10. Rintoul L, Panayiotou H, Kokot S, George G, Cash G, Frost R, et al. Fourier transform infrared spectrometry: a versatile technique for real world samples. *Analyst* 1998; 123: 571–577.
11. Chalmers JM, Everall NJ, Hewitsona K, Chesters MA, Pearson M, Grady A, et al. Fourier-transform infrared spectrometry: some advances in techniques for characterization and structure-property elucidations of industrial material. *Analyst* 1998; 123: 579–586.
12. Bhargava R, Wang S and Koening JL. FTIR microspectroscopy of polymeric systems. *Adv Polym Sci* 2003; 163: 137–191.
13. Eidelman N, Raghavan D, Forster AM, Amis EJ and Karim A. Combinatorial approach to characterizing epoxy curing. *Macromol Rapid Comm* 2004; 25: 259–263.
14. Corey EJ, Pasto DJ and Mock WL. Chemistry of Diimide. II. Stereochemistry of Hydrogen Transfer to Carbon-Carbon Multiple Bonds. *J Am Chem Soc* 1961; 83: 2957–2958.
15. Gaviglio C and Doctorovich F. Hydrogen-free homogeneous catalytic reduction of olefins in aqueous solutions. *J Org Chem* 2008; 73: 5379–5384.
16. Ratnayake WMN, Grossert JS and Ackman RG. Studies on the mechanism of the hydrazine reduction reaction applications to selected monoethylenic, diethylenic and triethylenic fatty-acids of cis configurations. *J Am Oil Chem Soc* 1990; 67: 940–946.
17. Katayama H, Kamigaito M and Sawamoto M. In-situ direct analysis of the growing species by 119 Sn NMR spectroscopy. *Macromolecules* 1998; 31: 4703–4709.
18. Mango LA and Lenz RW. Hydrogenation of unsaturated polymers with diimide. *Die Makromol Chem* 1973; 163: 13–36.
19. Lin X, Pan Q and Rempel GL. Modeling and simulation of diimide hydrogenation of nitrile butadiene rubber latex. *Ind Eng Chem Res* 2006; 45: 1300–1306.
20. Lin X. *Hydrogenation of unsaturated polymers in latex form*. Waterloo, ON, Canada: Chemical Engineering, University of Waterloo, 2005.